Signatures of collective local and nanoscale distortions in diffraction experiments

Angel J. Garcia-Adeva,[1, *] Dylan R. Conradson,[1] Phillip Villella,[1, 2] and Steven Conradson[1]

[1]*Materials Science and Technology Division (MST-8); Mailstop G755; Los Alamos National Laboratory; Los Alamos, NM 87545*
[2]*Department of Physics, University of Colorado, Boulder, Colorado 80309*

The effects of periodic and aperiodic distortions on the structure factor and radial distribution function of single-component lattices are investigated. To this end, different kinds of distortions are applied to the otherwise perfect square lattice and the corresponding radial distribution function and structure factor for the resulting lattices are calculated. When the applied distortions have a periodic character, they are very easily recognized in the calculated structure factors as new superlattice peaks. However, when the periodicity of the distortions is suppressed the signatures of disorder only show up as smooth and subtle features on the diffuse part of the scattering, making it very difficult to identify the nature of the distortions present in the lattice. The implications of these results are discussed.

PACS numbers: 61.46.+w, 61.43.-j, 61.72.-y

I. INTRODUCTION

Diffraction by X-rays (XRD) in the laboratory and at synchrotron facilities and neutrons at special sources are some of the most venerable experimental methods in Physics, having made a prominent contribution in establishing many basic concepts in atomic and solid state physics. In particular, our understanding of XRD is so profound that it is routinely used for obtaining structural information about crystalline solids. In conjunction with very powerful structural analysis algorithms, it is a matter of hours to identify the crystallographic positions of the atoms of an unknown crystalline material. However, diffraction analysis relies on the well-founded paradigm of crystalline solids as the periodic repetition of a small pattern of atoms (the unit cell). Even though this description of solids can be considered as one of the pillars in the construction of the modern condensed matter physics, it is also true that the vast majority of real solids exhibit one or another form of structural disorder. Aperiodic disorder manifests itself in the structure factor as diffuse scattering[1,2]. Although it is possible to extract information from the diffuse part of the scattering, the analysis is complicated and relies strongly on the particular structural model chosen. The possibility therefore exists for uniqueness problems that make it very difficult to gain reliable information about the disorder present in real solids. Thus, conventional crystallographic analysis of diffraction patterns provides an excellent description of the average long-range arrangements of the coherent fraction of the atoms, without providing definitive or even incisive information about local distortions that may be coupled to the compelling properties of many complex materials.

To put all these facts on a more formal basis, analysis of the Bragg peaks provides only information about the average positions, thermal disorder, and site occupancies. That it, conventional analysis of Bragg peaks provides a mean field description of the solid. In contrast, the diffuse part of the scattering contains information about two-point correlations and therefore can be a rich source of information about how pairs of atoms or molecules interact with each other. However, as we briefly mentioned above, extracting information from the diffuse scattering is still far from routine. Tradition-

ally, two main approaches have been used to understand the diffuse part of the diffraction pattern in the kinematic limit: The first is based on a real space formulation in terms of a set of short-range chemical and displacement pair correlations, which is specially useful when a small set of correlation parameters can describe the diffraction pattern and another one based on a reciprocal space formulation in terms of the modulations of the real space structure associated with sharp features in k-space. Obviously, this later approach is especially useful when sharp features are present in the diffuse part of the diffraction pattern. Aside from the fact that some of the approximations involved in the previous approaches are sometimes difficult to justify (i.e. retaining only the first few terms of a Taylor expansion), the main problem is that of uniqueness. As described above, diffuse scattering contains information only about the pair correlations. Therefore, many different atomic configurations can lead to the same set of pair correlations (while having very different higher order correlations, i.e., while representing completely different configurations) compatible with the set of parameters obtained from the analysis of the diffraction pattern by using these approaches, making the determination of the real structure of the material ambiguous. However, as very well put by Welberry and Butler[3], the ultimate goal of diffraction analysis is to obtain a realistic model of the structure of the material that is consistent with the observed diffraction pattern. In this sense, important progress has been done during recent years by using a method that, in some sense, is the converse of the aforementioned mathematical modeling. The idea is to develop a structural model that incorporates all the physical or chemical constraints already known from the system under consideration. This model is implemented in the computer (by using Monte Carlo methods) in such a way that the calculated diffraction pattern qualitatively agree with the experimental one and quantitative refinements of the model are iteratively implemented by taking into account the numerical constraints obtained from the aforementioned mathematical models. In this way, many unphysical configurations compatible with the diffraction data are discarded from the outset. In spite of the formidable computational requirements demanded by this approach, it has already shown its usefulness in analyzing and obtaining structural information of var-

ious systems, e.g., $Fe_3(CO)_{12}$[4], cubic stabilized zirconia, and disordered organic molecular crystals[1,3,5]. From these arguments, we can easily understand the importance of complementing conventional diffraction data with local probes, such as X-ray absorption fine structure (XAFS) measurements[6] and pair distribution functions (PDF). The long-range average order can be determined by using conventional analysis of the Bragg peaks while the local structure can be determined by using XAFS and PDF. This information about the local structure around each element can be used for constructing physical structural models that can be provided as input for the Monte Carlo methods for analyzing the mesoscale structural information contained in the diffuse scattering and to obtain pair distribution functions.

The necessity of using the previous hierarchical approach to the problem of determining the real structure of solids has become even more evident with the increasing realization that local lattice distortions may act collectively to produce nanoscale phase separation and heterogeneity (multiple different ordered domains), which are essential ingredients in understanding the physical properties of complex systems[7]. This is the case, for example, of substitutional impurities in solid solutions[8]. If the impurity atoms attract or repel each other, heterogeneous nanoscale domains or texture will be formed in the solid. Additional examples of these kinds of effects are charge separation and charge ordering in colossal magnetoresistance compounds high T_c superconductors leading to the formation of charge density waves and stripes[9,10,11,12,13,14]. These effects give rise to ordered electronic distributions that are easily observed in diffraction experiments as superlattice or satellite peaks.

However, the situation is radically different in the presence of aperiodic phase separation below the limit of "long" range order, i.e., when the structure of the solid cannot be simply described by the average positions of the atoms plus a small number of distortions. It is then necessary to consider a large number of correlation functions characterizing distortions and organization in many different length scales. In this case, the effects of heterogeneity, organization, and competition between different phases in the diffraction patterns are simply not known.

It may seem surprising that, in spite of the fact that it is widely accepted that some of the most compelling properties of real materials come from departures from perfect periodicity[30], there is a vast amount of literature concerned with describing theoretically how different types of disorder affect the diffuse part of the scattering[31], and that there is an increasing body of evidence[15,16,17,18,19,20,21,22,23,24,25,26,27] that suggest that the traditional interpretative frameworks based on the crystal picture of solids are not enough to understand the properties of complex systems, the signatures of disorder clearly seen in experimental diffraction data are, oftentimes, ignored.

One possible reason for this is that, sometimes, the situation in solids where nanoscale heterogeneity plays an important role can be even more complicated and misleading than the previous description may suggest and it is easier to rely on a well-established description of solids rather than carry on the

difficult and expensive program presented above. However, as we will prove in the present work, ignoring apparently small and unimportant features usually present in the diffuse scattering can lead us to develop models and extract conclusions from these models for systems that, simply put, have nothing to do with the real solid under consideration. Moreover, we will also show that, even in some extreme cases, aperiodic distortions affecting one fifth or more of the atoms in the lattice can barely affect the calculated structure factors when compared with their periodic counterparts, making it very easily to miss them by using conventional analysis methods. We will also see that even in some cases where distinct features of disorder are present, we can easily devise different types of distorted configurations that lead to qualitatively similar structure factors, making it very difficult to ascertain the nature of the underlying lattice. In order to develop this program, we will present the results of simulations of the structure factors and radial distribution functions (RDF) in lattices with different kinds of isolated and collective distortions. For simplicity, we have carried on the calculations in two-dimensional lattices. However, we do expect the conclusions drawn in this work to be extensible to the real three-dimensional case and the results of such an analysis will be reported elsewhere.

The remainder of this paper is organized as follows: In the next Section we will describe the lattices we have considered in this work. In Section III the results of our calculations for the RDF and structure factors, and a discussion of the main results are presented. Finally, Section IV is devoted to stating the conclusions of this work.

II. THE DISTORTED LATTICES

As briefly mentioned in the Introduction, we have considered 2D square lattices to which different kinds of static disorder have been applied in order to simulate various possible lattice distortions. For completeness, we have also considered purely periodic lattices obtained by distorting the square lattice (see below). The size of all the lattices reported in this work is 40×40 atoms (1600 atoms). This is a compromise between large enough lattices so the finite size effects are small while, at the same time, keeping the CPU time down to a reasonable amount (hours). Obviously, the finite size of the lattices will give raise to a broadening of the peaks in the calculated structure factors that makes it difficult to extract any conclusion about how these distortions affect the shape of the diffraction peaks. However, such an analysis of the shape of the peaks is outside the scope of this work and, besides, based on comparisons with the results for smaller lattices, this broadening does not modify any of the conclusions reached in this work about the effects of distortions on the diffuse scattering. The lattice parameter used in all the calculations is 3 Å. Let us now briefly review the different kinds of distortions that have been applied to the otherwise perfect square lattice:

- The first case we have considered consists of different configurations of vacancies placed on the square lattice (see Fig. 1). The first and simplest configuration of

vacancies consists on randomly removing 20% of the atoms of the lattice in order to test the effect of random, aperiodic elimination. In addition, we have also considered configurations in which the positions of the vacancies are not random, but correlated, forming channels across the lattice and periodic and aperiodic distributions of vacancies defining certain regular geometric shapes. Finally, we have also considered a configuration in which the vacancies define different regular shapes which are randomly placed in the lattice.

- Atoms displaced from their original crystallographic positions (Fig. 2). The configurations considered in this case are similar to the previous ones. The first type of displacements we have considered consists on randomly choosing a 20% of the atoms of the lattice and displacing them by a vector $(\cos\theta, \sin\theta)$, where θ randomly varies among $32°$, $148°$, $212°$, and $328°$ (see Fig. 2(a)). The second type of displacements we have considered is similar to the channel of vacancies explained above, except for the fact that now, instead of removing the atoms, they are displaced by the same random vector as in the previous displaced configuration (see Fig. 2(b)). We have also considered the case in which a certain number of atoms defining a regular shape (a small cross) are displaced by the same random vector, and this shape is periodically and aperiodically repeated across the lattice (see Figs. 2(c) and 2(d)). Finally, we have also tested the effect of having two phases of different symmetries inside the lattice. To this end, the interatomic distances between the atoms defining the crosses used in the last two configurations have been contracted by a factor $0.04a$ in the horizontal direction. These two configurations have not been depicted, at the visual differences with respect to the last two cases are barely noticeable.

- Inclusion of a tetragonal domain. We have considered the effect of contracting a regular domain (a square domain) in the horizontal direction by an amount $0.04a$ (see Fig. 3). In order to see what is the minimum size this domain has to be, in order to show up in the $S(Q)$, different domain sizes have been considered, ranging from 4×4 atoms up to 40×20 atoms (half the lattice is contracted). Additionally, we have also considered a lattice in which the positions of groups of atoms defining a geometric motif (a small cross), randomly placed in the lattice, have been tetragonally distorted (see Fig. 3(b)).

- Periodic and aperiodic modulated distortions (Fig. 4). Each of the elementary square cells in the lattice is assigned a position vector of the form (i, j), where i and j are both integer numbers. For example, the (1,0) cell would correspond to the cell defined by the atoms located at (0,0), (0,a), (a,0), and (a,a). In order to implement this kind of distortion, in the periodic case, the positions of all the atoms on the corners of the cells with odd i and j have been shifted towards the center of the

corresponding cell by a 4% of the undistorted lattice parameter (see Fig. 4(a) for details). The resulting lattice can be seen as another square lattice of lattice parameter $2a$ with a basis. In the aperiodic case (Fig. 4(b)), the procedure is similar to the periodic case, but we have allowed the direction of the contraction to randomly vary among the values $25°$, $45°$, and $65°$.

- Periodic and aperiodic interstitial atoms. Using the periodic modulated lattice described in the previous paragraph, an interstitial atom has been placed inside each of the squares defined by those atoms with largest bondlength (see Fig. 5). In the periodic case, the interstitial atom is located in the center of the square. Again, this new lattice can be seen as a square lattice of lattice parameter $2a$ with a basis. In the aperiodic case, the interstitial atom is randomly located in a circle of radius $0.04a$ centered at the middle point of the square (see Fig. 5(b) for details).

- Periodic and aperiodic channels of defects across the lattice. In this case, the effect of correlated networks of defects has been studied. In the periodic case, all the atoms belonging to a chosen column have been shifted downwards by half the lattice parameter. At the same time, the atoms belonging to this channel have been shifted in the horizontal direction by an amount $\frac{a}{6}$ or $-\frac{a}{6}$, respectively (see Fig. 6(a)). In addition, each seventh atom in the network has been removed. Finally, the distorted network has been periodically repeated across the horizontal direction. In the aperiodic case, channels across the lattice similar to the ones introduced in the case of vacancies and displacements have been considered (see Fig. 6(b)). However, in contrast with the displacements case, the atoms inside this channel have been alternatively displaced horizontally or vertically, in such a way that they define a second tetragonal phase inside the square lattice, whereas in the displacements case, the displacements where applied in a random fashion. Moreover, each seventh atom has been removed.

As stated in the Introduction, our intention is to study how these different types of distortions affect the calculated diffraction patterns. The result of this analysis is presented in the next Section.

III. RESULTS AND DISCUSSION OF THE CALCULATED STRUCTURE FACTORS AND RADIAL DISTRIBUTION FUNCTIONS

The static structure factor (SF) $S(Q)$ and radial distribution function (RDF) $g(r)$ have been calculated for the lattices introduced in the previous Section. To this end, we have used the code CRYGEN2D, developed by P. Villella and coworkers at Los Alamos National Lab[28]. This program takes as input the coordinates of the atoms in a two-dimensional lattice and exactly computes the RDF and $S(Q)$. For comparison, the $S(Q)$ and $g(r)$ of a 40×40 atoms square lattice have

been also calculated, and used as reference. In order to simulate the effects of finite temperature, we have used a typical Debye-Waller vibrational factor of amplitude 0.05 Å. The $S(Q)$ data have been normalized in order to eliminate differences coming from the different number of atoms present in some lattices with respect to the square one. This allows us to compute the difference between any two $S(Q)$ data sets, so the differences in the diffuse scattering are more noticeable. The results of the $S(Q)$ calculations are presented below in terms of the dimensionless variable $\left(\frac{Q\,a}{2\pi}\right)^2 = h^2 + k^2$ (with h and k the Miller indices), which makes it very simple to assign the Bragg peaks. Let us now review how these different kinds of distortions affect the calculated $g(r)$ and $S(Q)$.

Effect of random vacancies.- The results for the RDF and $S(Q)$ can be seen in Fig. 7. As one would expect, the only effect of vacancies on the RDF is a reduction in the intensity of the peaks proportional to the concentration of vacancies in the lattice.

The situation is a little more complicated for the calculated structure factors. The fundamental peaks are located at the same positions as for the square lattice and have the same shapes. Their intensities, however, are smaller for the lattices with vacancies than for the square lattice due to the fact that part of the intensity goes now to the diffuse part of the scattering. For the case of 20% atoms randomly removed from the lattice, the main effect is an increment of the background, very similar to the effect of a Debye-Waller factor, except for the fact that this background is essentially constant for all Q's, in contrast to the Debye-Waller diffuse scattering, which is larger for larger values of Q. In the case of the channels of vacancies extending through the lattice, the main effect is an increment of the diffuse scattering around the $[i\,0]$ $(i = 1, 2, 3, \dots)$ peaks. This enhancement is highly asymmetric, affecting only the high-Q part of the peak.

If we now turn our attention to the configurations in which vacancies define geometric shapes, we can see that, in the periodic case, many new peaks appear at incommensurate positions with respect to the spacing of the original square lattice. Obviously, these new peaks are nothing but superlattice peaks associated with the fact that the lattice can still be seen as a square lattice of lattice parameter $10a$ with a complicated basis. We will further comment on these superlattice peaks below. In contrast, if these shapes are randomly distributed, the superlattice peaks disappear, and the background acquires an modulated character: there is an enhanced diffuse scattering around the fundamental peaks, and this background is depleted in between. The combination of these two effects give rise to some kind of oscillatory diffuse scattering. This effect is more noticeable at low Q. We wanted to check if these oscillations were due to the fact that all the defects have the same size and shape and, to this end, we repeat this calculation using different shapes and sizes, but located at the same positions (see Fig. 1(e)). As can be seen from the green curve in the lower panel of Fig. 7(b), this is not the case, and the only difference between these two configurations is a barely noticeable increment of the diffuse scattering around the fundamental peaks at larger Q, in this last case.

Effect of aperiodic displacements.- The results for this case can be seen in Fig. 8. The RDF for the distorted lattices shows the original peaks of the square lattice (the intensity of these peaks is reduced, as expected) plus additional new peaks due to the new pairwise distances introduced by the displaced atoms. The new distances are especially apparent in the RDF for the lattice in which 20% of the atoms are randomly chosen and shifted from their crystallographic positions. For example, if we consider the peak corresponding to the nearest neighbor (NN) distances, we can see that four new peaks corresponding to the four new NN distances introduced by the distortions. The intensity of these new peaks are the same, as each of the four displacement vectors are equally probable. Similar comments apply to further neighbor peaks. The other configurations exhibit exactly the same features as this last one: The same new peaks appear and they are located at the same positions. The main difference is the intensity of the new peaks which, obviously, is higher for those configurations involving a larger number of atoms displaced (320 atoms in the case of the 20% randomly chosen atoms to be compared with 200 in the channel case and 192 for the shifted crosses, respectively). This reduction in the intensity of the peaks is especially noticeable in those configurations in which the displaced atoms define a regular shape, as in this case the only new distances are located at the interface between the displaced and undistorted lattice. When additional tetragonal contractions are applied to these shapes, there are also new distances between the atoms defining the shape itself (for example, the NN distance in the horizontal direction is now 2.88 Å). However, these new distances are masked by the thermal broadening of the peaks associated with the regular part of the lattice.

The situation is more complicated for the calculated $S(Q)$. The intensity of the fundamental peaks decreases as part of it goes into additional structure appearing in the diffuse part of the scattering. For the configuration in which 20% of the atoms are randomly chosen and shifted, the background scattering exhibits modulated variations (enhanced background at low Q, depleted at intermediate values, and enhanced again at high values of Q), giving the impression of an oscillatory background, clearly different from the effect of purely thermal disorder. For the channel of displaced atoms, the behavior of the diffuse scattering is very similar to that of the channel of vacancies discussed above: The high-Q part of the $[i\,0]$ $(i = 1, 2, 3, \dots)$ reflections is enhanced. For comparison, we have depicted the difference between the $S(Q)$ for this configuration and the one for the channel of vacancies (the violet curve in the bottom panel of Fig. 8(b)). As can be seen from that curve, the only difference between the $S(Q)$ for these two configurations is the intensity of the fundamental reflections. For other values of Q this curve is essentially a flat line.

If we now turn our attention to the configurations where the shifted atoms define geometrical shapes, we can observe from Fig 8(b) that the results for those cases in which the regular shapes are periodically chosen and then randomly shifted (both with and without tetragonal contraction) are very interesting: The resulting $S(Q)$ resembles that of a periodic lat-

tice (appearance of superlattice peaks at incommensurate $[h\,k]$ values), even though there does not exists an elementary motif (unit cell) from which the whole lattice can be obtained by periodic repetition. When these shapes are randomly distributed, the resulting diffuse scattering lacks any sharp features and, instead, it exhibits an oscillatory character with enhanced diffuse background around the fundamental reflections and depleted in between. Strikingly, the calculated SFs for both the regular shapes with and without tetragonal contractions are essentially identical, as can be seen from the green and brown curves in the bottom panel of Fig. 8(b), which are essentially flat lines. These observations imply that, even though we can induce the presence of a random or ordered motif of defects, it is difficult to judge whether this motif contains no atoms at all or a phase with a symmetry completely different from the one of the initial lattice. We will further develop this point when stating the conclusions of this work.

Effect of the inclusion of a tetragonal domain.- The results of the calculations for this type of distortions can be seen in Fig. 9. In that figure, we have only depicted the results for some representative domain sizes. For the sake of comparison, the $S(Q)$ for a 40×40 lattice tetragonally contracted in the horizontal direction is also shown. As stated above, we also show in that figure the results RDF and $S(Q)$ for the lattice depicted in Fig. 3(b), where randomly placed regular shapes have been horizontally contracted. The RDF for those lattices with a single tetragonal domain nicely interpolates between the one for the square lattice and the one of a purely tetragonal lattice, and peaks associated to the new distances inside the tetragonal domain clearly develop as the domain size increases. It is interesting to note, though, that for practical purposes, below a domain size of 12×12 atoms, the new distances are barely noticeable in the RDF. The RDF for the randomly distributed tetragonally contracted shapes is very similar to the one consisting of a single tetragonal domain with the same number of atoms with the only difference of some small and broad peaks occurring at higher distances associated to the distances between the boundaries of the geometrical shapes and the atoms in the square phase.

Regarding the $S(Q)$, we can see in Fig. 9(b) that new peaks, typical of the tetragonal symmetry, develop as the domain size is increased. Interestingly, these peaks are only noticeable for large domain size and, even for the 40×20 domain, the tetragonal peaks are not fully developed. However, the resulting $S(Q)$ for this lattice is fully consistent with the one obtained by adding up the $S(Q)$ for a square 40×20 lattice plus the one for a 40×20 one. Furthermore, the positions of the fundamental reflections are shifted to higher Q, due to an overall (though small) contraction of the lattice. Even though we have not shown it in that figure, we found that for sizes smaller than 12×12 atoms the new peaks are barely noticeable. The $S(Q)$ for the lattice with tetragonal shapes randomly distributed is essentially identical to the one of the square lattice, as can be seen in the lower panel of Fig. 9(b).

Effect of periodic and aperiodic modulated distortions.- The results of the calculations for this type of distortions can be seen in Fig. 10. The RDF for the modulated lattices (both periodic and aperiodic), are quite distinct from the square lattice

one, as new distances are generated in the distorted lattices. As a result of these distortions, some of the peaks (noticeably the ones corresponding to NN, next NN, 6th NN, and 7th NN) are split reflecting these new distances, whereas in other cases (3rd, 4th, and 5th NN) the only effect is an additional (small) broadening superimposed to the thermal one. We can also see that the RDF for the aperiodic lattice is very similar to the periodic one, as we could expect from the fact that the distortions we have implemented average out to zero. The only noticeable difference is an slight additional broadening of the split peaks.

The $S(Q)$ for these lattices shows interesting features again. In the periodic case, many new small superlattice peaks at incommensurate h and k values appear associated with the fact that the modulated lattice is another square lattice of parameter $2a$ with a basis. The interesting point, however, is that the $S(Q)$ for the aperiodic modulated lattice is almost identical to the periodic one, as can be seen from the curve labeled "Differences" in the lower panel of Fig. 10(b). The only noticeable difference is the appearance of a marginal amount of diffuse scattering close to the fundamental reflections. Moreover, in both the periodic and aperiodic cases, the original peaks are only minimally affected until $h^2 + k^2 \approx 16$.

Effect of periodic and aperiodic interstitial atoms.- The results of the calculations for these types of lattices can be seen in Fig. 11. Regarding the RDF calculation, new distinct peaks appear associated with the new atom in the basis (see Fig. 11(a)), when compared with the calculated RDF for modulated lattice described above . This is especially clear in the periodic case. In the aperiodic case, these same peaks remain, but they are broadened by disorder, as expected.

Regarding the results for the $S(Q)$, this quantity exhibits the peaks already described in the modulated lattice case plus new superlattice peaks associated with the sublattice of interstitial atoms. However, in full analogy with the previous case, the $S(Q)$ for the aperiodic case is essentially identical to the periodic one, the difference between this two cases being again a slight increment of the diffuse scattering around the fundamental peaks. When compared with the same curve for the modulated lattice the only difference is that the differences in the diffuse scattering around the fundamental reflections slightly increase at higher Q.

Effect of networks of tetragonal distortions across the lattice.- The results of the calculations for these lattices can be seen in Fig. 12. The main effect of these distortions in the RDF is to produce many new peaks associated with the new pair distances inside the tetragonal channels. Interestingly, there are no noticeable differences between the periodic and aperiodic cases. This is not the case, however, for the $S(Q)$. The periodic channels give rise to new superlattice diffraction peaks as happened in all the cases where the distortions where periodic. When the periodicity is removed, these superlattice peaks disappear and there is an enhancement of the diffuse scattering localized around the fundamental peaks of the square lattice, even though the RDFs for both lattices were essentially identical. It is interesting to notice that this enhancement of the diffuse scattering is somewhat similar to the one observed for the channel of vacancies and channel of ran-

dom displacements. However, in this case the enhancement only occurs at the high-Q part of the $[i\,0]$ reflections, with i *an odd integer*. For completeness, we have included the differences between the $S(Q)$ for the aperiodic channel of tetragonal distortions (Fig. 6(b)) and the ones for the channel of vacancies (Fig. 1(b)) and the channel of aperiodic displacements (Fig. 2(b)) in the lower panel of Fig. 12(b). Apart from differences in the relative intensities of the fundamental peaks, the main difference occurs, obviously, around the high-Q part of the $[i\,0]$ reflections, for the reasons commented above. The rest of the diffuse scattering is essentially the same for the three lattices.

A. A comment on the superlattice peaks

Throughout this work, we have consistently observed that the effect of periodic lattice distortions on the calculated structure factors is the appearance of localized peaks, with very small intensities, at incommensurate values of the Miller indices. We have denoted these peaks as *superlattice peaks* or *superlattice reflections*, extending the common usage of these terms that are usually used for non-stoichiometric compounds with chemical disorder[2], to the present mono-component lattices. In fact, these satellite peaks appearing in our calculations for periodically distorted lattices are nothing but Bragg peaks and the reason why they appear at incommensurate positions in the previous figures is because of the *naive* (and intentional) way in which the unit cell for those lattices was chosen. To see this, let us consider two representative examples, namely, the periodically modulated lattice (Fig. 4(a)) and the lattice with periodic channels of tetragonal distortions (Fig. 6(a)). For the modulated lattice it is easy to see that the resulting distorted lattice can be described as another square lattice in which the smallest motif that generates the whole lattice is another square unit cell of lattice parameter $2a$ with a basis of 4 atoms. For the channel of tetragonal distortions, the elementary motif is another square lattice of lattice parameter $7a$ with a basis of 58 atoms. If we now use the correct values for the size of the unit cell we will obtain results as the ones depicted in Fig. 13. As we can see, what seemed to be satellite peaks at incommensurate positions in h and k are nothing but Bragg reflections occurring at the same positions as the ones of the square lattice. Of course, the relations between the intensities of these peaks are completely different from the ones for the simple square lattice, due to the relative positions of the atoms inside the unit cell. Actually, these geometrical relations lead in some cases to a cancellation of the intensity of some peaks, what is usually called an *extinction* of the peak. This is especially noticeable in these examples for the modulated lattice, in which all the peaks with both h and k odd are absent, those with mixed h and k are almost extinct, and the relative intensities of the peaks with both h and k even are unaffected. The analysis for the lattice with periodic channels of tetragonal distortions is more complicated. To begin with, the original 40×40 lattice considered in this work contains only 5×5 periodic unit cells[32]. Thus, the shapes and intensities of the peaks at very low Q are extremely affected by the

finite size of the lattice and the intensities of these peaks are of the same order of magnitude as the oscillatory tails of the Bragg peaks (which are also associated to the finite size of the lattices), making it very difficult to distinguish among them. For this reason, we repeated the calculation for a bigger lattice containing 13×13 unit cells (which amounts to 9802 atoms) and reduced the interatomic distance of the undistorted lattice to 1 Å. In doing so, the Bragg peaks are easily distinguished from the oscillatory tails. The result of this calculation shows again that the satellite peaks of Fig. 12(b) are nothing but Bragg peaks when a truly periodic unit cell is chosen. Furthermore, all the reflections are present in this case. The main effect of the complicated basis is that the intensity ratios of the reflections are completely different from the corresponding ones for the square lattice.

Obviously, we have not said anything new in this subsection, as all these facts have been known for a long time[29]. However, we think it is worthy to stress this point, as it seems that other authors at times forget to mention these elementary facts when analyzing diffraction patterns of lattices with periodic distortions.

IV. CONCLUSIONS

This work is concerned with the effects of certain types of static distortions, both periodic and aperiodic, local and collective, in the diffraction patterns of materials. Starting from a 2D square lattice, we have implemented different kinds of distortions to obtain new, periodic or aperiodic, 2D lattices. The radial distribution functions and structure factors for these lattices have been computed. The main result coming from the calculations is that periodic distortions are easily identified in the structure factors as new superlattice peaks or, equivalently, as extinction of certain Bragg reflections or changes in the relative intensities when the correct unit cell is chosen, as is known. When the periodicity of the distortions is lost, there are also some signatures present in the $S(Q)$, for example, an enhanced and asymmetric diffuse background around the fundamental peaks of the original lattice or oscillations of this same background. However, it is very difficult, if not impossible, to assess the exact nature of these distortions (i.e. whether they are vacancies or random displacements, for example). This fact is nothing but the realization, for the particular examples presented in this work, of the aforementioned uniqueness problem in the determination of the real structure of a material taking as a starting point the diffraction pattern.

It is important to stress at this point that the experimental situation can be even more misleading than the results presented in this work, as experimental measurements are always subject to additional effects we have not taken into account in our simulations. These include limited Q resolution, instrumental broadening, and noise. Instrumental broadening, especially, can very easily mask some of the peak splittings we obtain in our calculations. Regarding the calculated radial distribution functions, in some cases we have seen that they provide more intuitive information than the $S(Q)$ for the kinds of distortions considered in this work. This fact strongly

supports the idea that PDF measurements can be crucially important in making progress in the problem of the determination of the structure of complex systems. However, this approach is not exempt to limitations. On one hand, it is necessary to use very intense sources in order to be able to measure the diffraction pattern up to very large values of Q (~35–45 Å^{-1} typically). Fortunately, with the availability of very intense synchroton and neutron sources this problem is partially alleviated, and these wave-vectors are experimentally achievable. On the other hand, the main limitation in extracting information from experimentally (Fourier-transformed diffraction data) determined pair distribution functions is the effect of thermal broadening that can very easily mask some of the features associated to local distortions. We have seen some examples of this problem when studying the effects of small domains with tetragonal distortions in the radial distribution function: the new peaks associated with the new, shorter distances of the tetragonal phase are closer to the peaks associated to the pair distances of the square lattice than the width of those peaks, making it very difficult to distinguish them. What is even worse, the radial distribution function is completely oblivious to certain kinds of distortions (as it happened with the vacancies configurations). It is in these situations where X-ray absorption fine structure could play an important role, as this type of probe is sensitive to local distortions and to the different species present in the sample. The main limitation in this case is associated to the fact that the XAFS spectra contain multiple scattering contributions and, thus, the kinematic limit is not applicable to the analysis of the data, making it extremely difficult to extract information about the radial distribution at long distances from the probed atom.

We also want to emphasize that, obviously, we are aware of the fact that the kind of distortions we have studied in this work hardly exist in real materials. They are simple illustrative examples of how easy it is to miss important structural information about local and collective distortions if we blindly trust structural models obtained by only applying conventional diffraction analysis methods. Our intention is to motivate awareness about this potential problem. The emerging picture of complex solids strongly supports the idea that local and nanoscale distortions exist (probably even more complicated ones than the toy models we have studied in this work), there are mechanisms that make them stable, and they play an important role in the properties of these systems. However, as has been shown throughout this work, the signatures of such aperiodic distortions are subtle and misleading interpretations can be reached if special care is not paid to their analysis.

We think that the above paragraphs serve to further stress the point already made in the Introduction: It is necessary to use a combination of experimental methods that probe all the relevant length scales (x-ray and neutron diffraction experiments, XAFS, PDF, etc). At the same time, a combination of structural analysis methods (PDF analysis, reverse Monte Carlo simulations, etc), beyond the standard Rietveld analysis, is necessary in order to reach a consistent picture of the structure of complex solids that can lead us to understand and exploit their properties.

* Electronic address: angarcia@lanl.gov

[1] T.R. Welberry and B.D. Butler, Chem. Rev. **95**, 2369 (1995)

[2] B.E. Warren, *X-Ray Diffraction* (Dover, New York, 1990)

[3] T.R. Welberry and B.D. Butler, J. Appl. Cryst. **27**, 205 (1994)

[4] T.R. Welberry, Th. Proffen, and M. Bown, Acta Cryst. **A54**, 661 (1998)

[5] T.R. Welberry, Acta Cryst. **A54**, 244 (2001)

[6] S. D. Conradson, Applied Spectroscopy **52**, A252 (1998)

[7] Proceedings of the *Local and Nanoscale Structure in Complex Systems 2002* conference. S.D. Conradson, ed. (to be published in Journal of Nanoscience and Nanotechnology)

[8] G.E. Ice and C.J. Sparks, Annu. Rev. Mater. Sci. **29**, 25 (1999)

[9] Z.A. Xu, N.P. Ong, Y. Wang, T. Kakeshita, and S. Uchida, Nature **406**, 486 (2000)

[10] J. Zaanen, Nature **404**, 714 (2000)

[11] A. Moreo, S. Yunoki, and E. Dagotto, Science **283**, 2034 (1999)

[12] E. Dagotto, T. Hotta, and A. Moreo, Phys. Rep. **344**, 1 (2001)

[13] J.M. Tranquada, B.J. Sternlieb, J.D. Axe, Y. Nakamura, and S. Uchida, Nature **375**, 561 (1995)

[14] J. M. Tranquada, K. Nakajima, M. Braden, L. Pintschovius, and R. J. McQueeney, Phys. Rev. Lett. **88**, 075505 (2002)

[15] A. Bianconi, N. L. Saini, A. Lanzara, M. Missori, T. Rossetti, H. Oyanagi, H. Yamaguchi, K. Oka, and T. Ito, Phys. Rev. Lett. **76**, 3412 (1996)

[16] N. L. Saini, H. Oyanagi, A. Lanzara, D. Di Castro, S. Agrestini, A. Bianconi, F. Nakamura, and T. Fujita, Phys. Rev. B **64**, 132510 (2001)

[17] A. Bianconi, Int. J. Mod. Phys. B **14**, 3289 (2000)

[18] P. Villella, S. D. Conradson, F. J. Espinosa-Faller, S. R. Foltyn, K. E. Sickafus, J. A. Valdez, and C. A. Degueldre, Phys. Rev. B **64**, 104101 (2001)

[19] F. J. Espinosa, P. Villella, J. C. Lashley, S. D. Conradson, L. E. Cox, R. Martinez, B. Martinez, L. Morales, J. Terry, and R. A. Pereyra, Phys. Rev. B **63**, 174111 (2001)

[20] F. J. Espinosa, J. M. de Leon, S. D. Conradson, J. L. Pea, and M. Zapata-Torres, Phys. Rev. B **61**, 7428 (2000)

[21] T. A. Tyson, J. M. de Leon, S. D. Conradson, A. R. Bishop, J. J. Neumeier, H. Rder, and J. Zang, Phys. Rev. B **53**, 13985-13988 (1996)

[22] G. G. Li, F. Bridges, J. B. Boyce, T. Claeson, C. Strom, S.-G. Eriksson, and S. D. Conradson, Phys. Rev. B **51**, 8564 (1995)

[23] L. E. Cox, R. Martinez, J. H. Nickel, S. D. Conradson, and P. G. Allen, Phys. Rev. B **51**, 751-755 (1995)

[24] G. G. Li, J. Mustre de Leon, S. D. Conradson, M. V. Lovato, and M. A. Subramanian, Phys. Rev. B **50**, 3356-3362 (1994)

[25] W. Dmowski, R. J. McQueeney, T. Egami, Y. P. Feng, S. K. Sinha, T. Hinatsu, and S. Uchida, Phys. Rev. B **52**, 6829 (1995)

[26] L. Vasiliu-Doloc, S. Rosenkranz, R. Osborn, S. K. Sinha, J. W. Lynn, J. Mesot, O. H. Seeck, G. Preosti, A. J. Fedro, and J. F. Mitchell, Phys. Rev. Lett. **83**, 4393 (1999)

[27] S. Shimomura, N. Wakabayashi, H. Kuwahara, and Y. Tokura, Phys. Rev. Lett. **83**, 4389 (1999)

[28] P. Villella, D. Dimitrov, and S.D. Conradson (unpublished); P. Villela, PhD Thesis (unpublished).

[29] N. W. Ashcroft and N. D. Mermin, *Solid State Physics* (Saunders, Philadelphia, 1976)

[30] See for example Ref. 8 and references therein.

[31] See for example the extensive bibliography presented in Ref. 1.

[32] And the lattice is not truly periodic. It is interesting to notice that the $S(Q)$ does not reflect this fact.
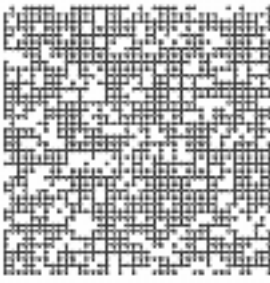
(a) Vacancies randomly placed in the lattice
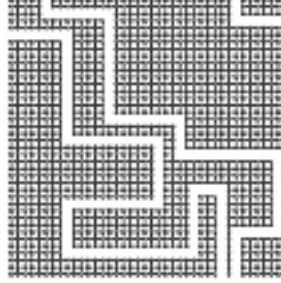
(b) Vacancies forming channels accross the lattice
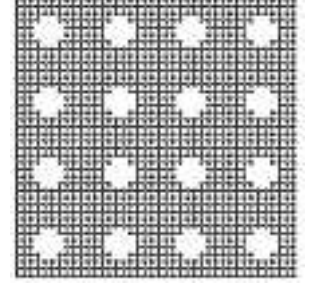
(c) Vacancies forming a regular shape which is distributed in an ordered fashion
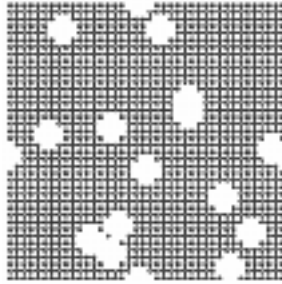
(d) Vacancies forming a regular shape which is randomly placed on the lattice
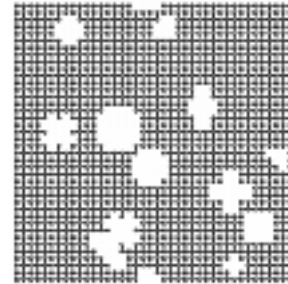
(e) Vacancies forming different shapes which are randomly placed on the lattice

Figure 1: The configurations of vacancies considered in this work.
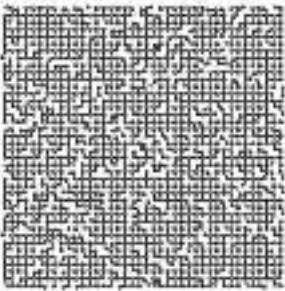
(a) Randomly selected atoms
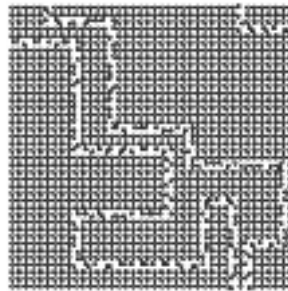
(b) Channel of displacements
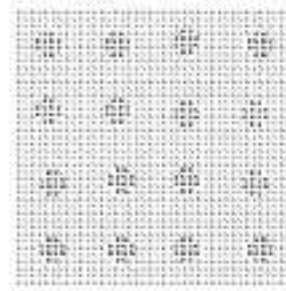
(c) Atoms forming regular shapes which are shifted as described in the text
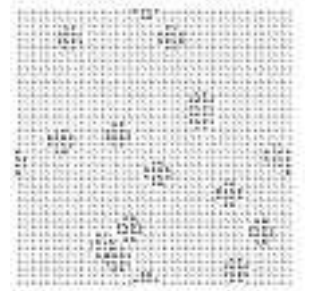
(d) Atoms forming regular shapes randomly placed in the lattice which are shifted as described in the text

Figure 2: Lattices with atoms displaced from their crystallographic positions. As explained in the text, we have also considered two additional cases not depicted here, analogous to cases (c) and (d), where the small crosses are additionally contracted an amount $0.04a$ in the horizontal direction.

(a) Single tetragonal domains

(b) Randomly placed tetragonal domains
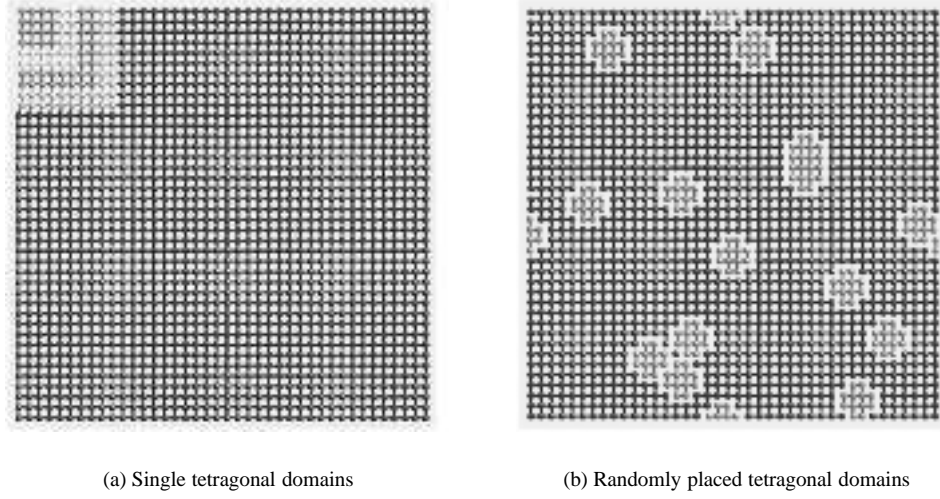
Figure 3: Inclusion of tetragonally distorted domains in the square lattice. In (a), we have shaded with different grays some of the domains considered in this work, in particular, 4×4, 6×6, 8×8, and 10×10 atom domains. In (b), the interatomic distances of the atoms belonging to the small crosses are contracted by an amount $0.04a$.

(a) Periodic modulated distortions.

(b) Aperiodic modulated distortions.
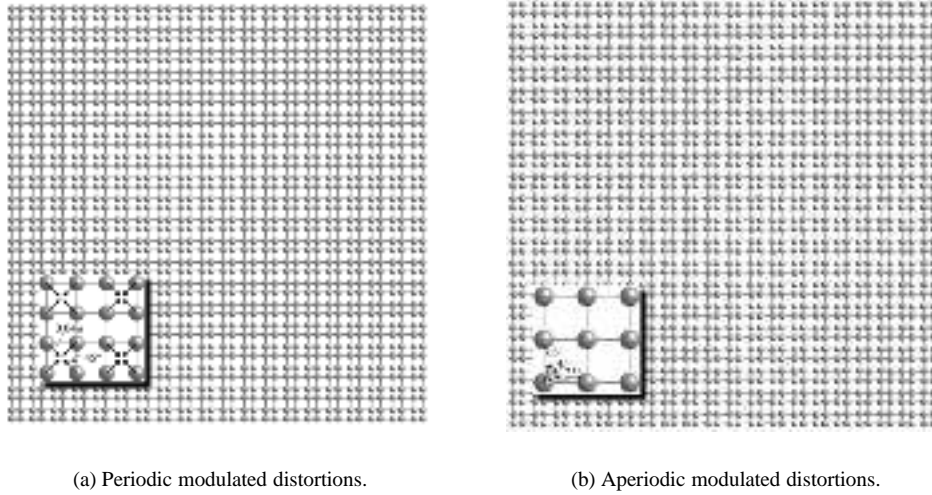
Figure 4: Modulated lattices. The insets show how the distortions are implemented in both the periodic and aperiodic cases.
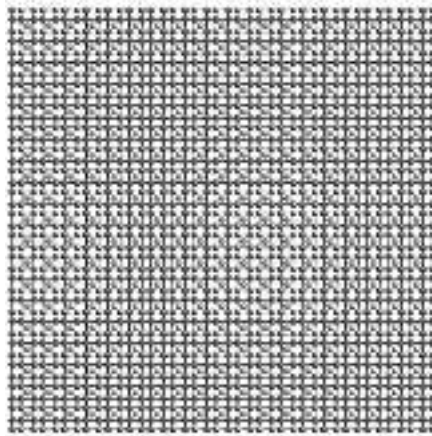
(a) Periodically distributed interstitial atoms
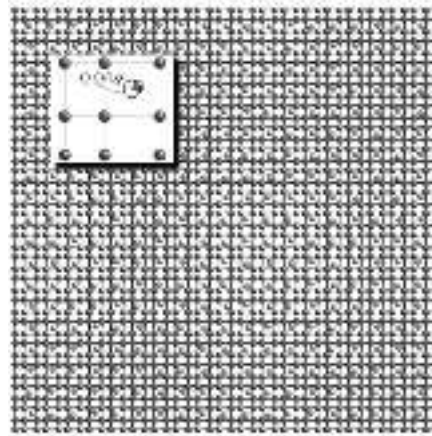
(b) Aperiodically distributed interstitial atoms

Figure 5: Lattices with interstitial atoms. The inset in figure (b) shows how the interstitial atoms are placed on the lattice in the aperiodic case. They are placed on a randomly chosen point of the circumference with center at the center of the cell and radius $0.04a$.
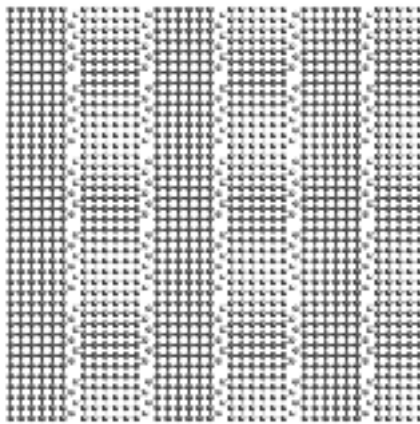
(a) Ordered periodic channels
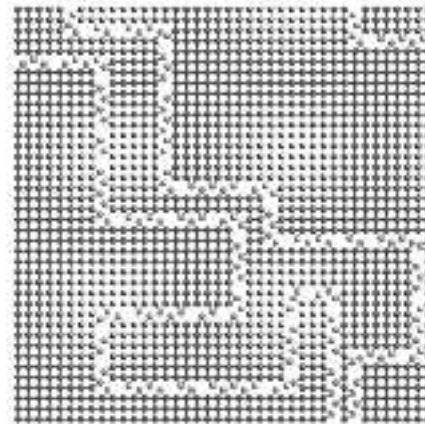
(b) Aperiodic channels

Figure 6: Lattices with channels of tetragonal distortions.

(a) Radial distribution function

(b) Structure function
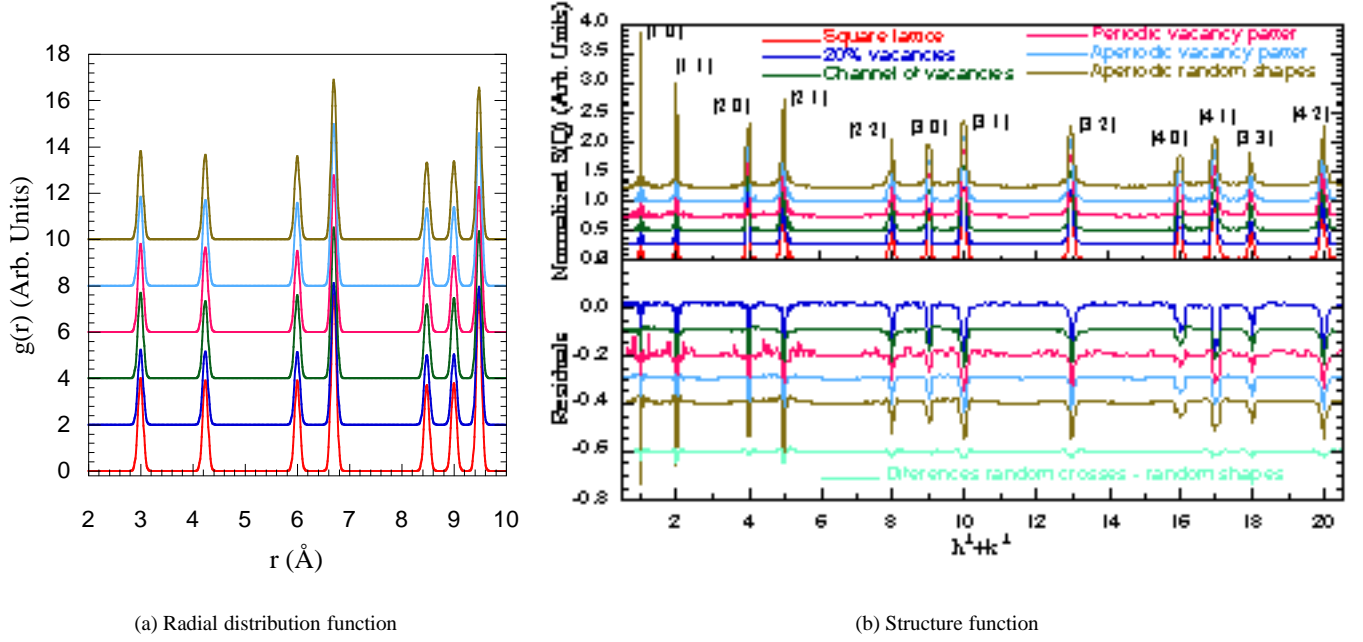
Figure 7: RDF and $S(Q)$ for the lattices with vacancies. The assignments of the diffraction peaks of the square lattice are shown in the upper panel of (b) for reference. The lower panel shows in greater detail the difference between the $S(Q)$ of the square lattice and the ones of the distorted lattices. In order to construct these curves, the $S(Q)$ have been properly normalized and the $S(Q)$ of the square lattice has been subtracted from the rest of $S(Q)$ of the distorted lattices. The units used in that panel are the same as the ones used in the upper panel. In this way, negative values correspond to regions in which the $S(Q)$ of the square lattice is larger than the corresponding one for the distorted lattice. As expected, peaks with negative values occur at the positions of the fundamental peaks of the square lattice diffraction pattern, whereas peaks with positive values correspond to additional features coming from the distorted character of the lattices (superlattice peaks or diffuse scattering). The green curve labeled "Differences random ... " has been obtained by subtracting the $S(Q)$ of the lattice in Fig. 1(e) from the one of the lattice depicted in Fig. 1(d).
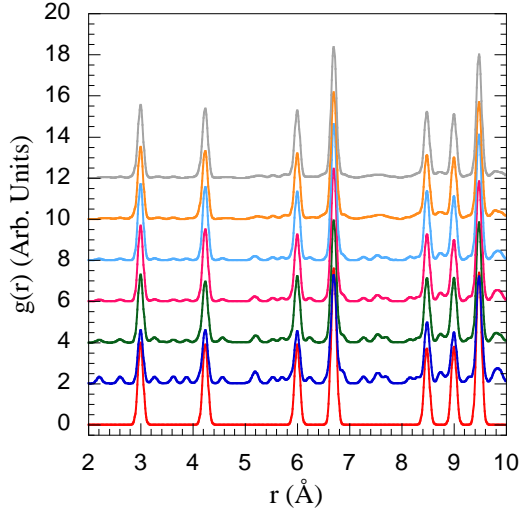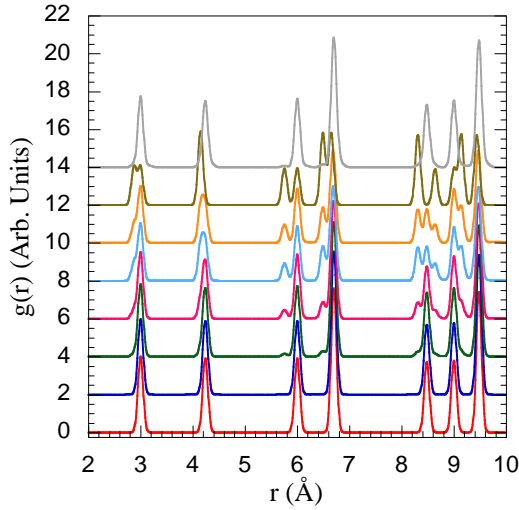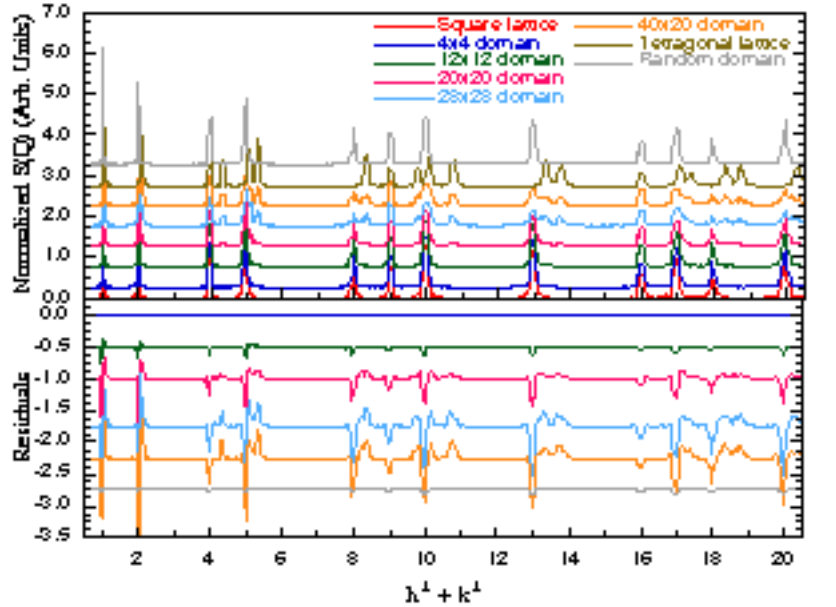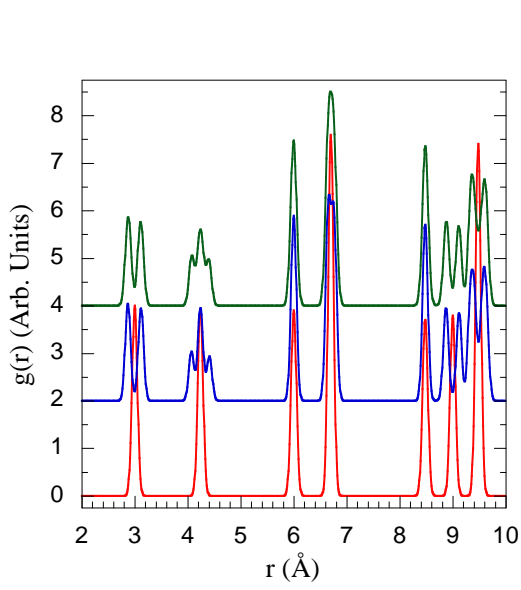
(a) Radial distribution function
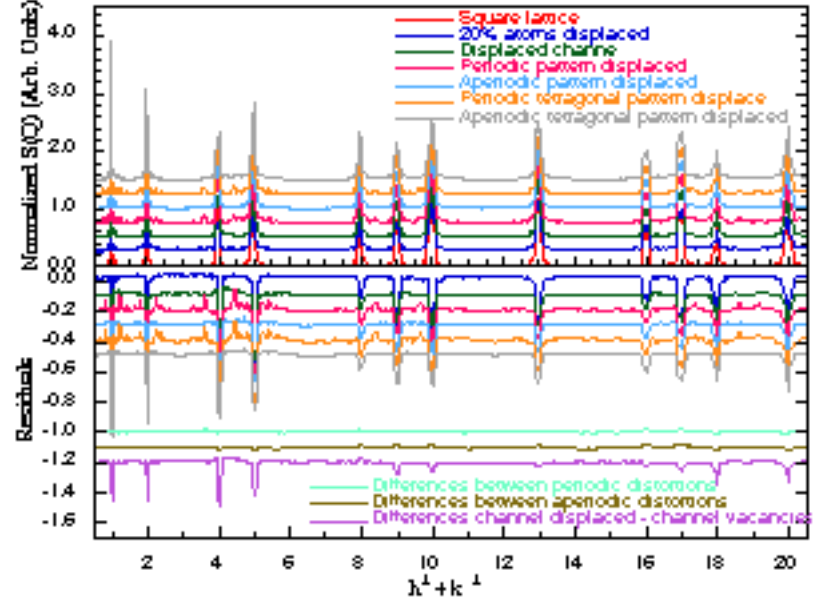
(b) Structure factor

Figure 8: RDF and $S(Q)$ for the lattices with displacement distortions. See the comments in the caption of figure 7 about how the lower panel has been constructed. The curve labeled "Differences between periodic distortions" has been calculated by subtracting the $S(Q)$ of the lattice depicted in Fig. 2(c) to the one of the analogous lattices where additional tetragonal contractions have been applied to the small crosses distributed in an ordered fashion in the lattice. The same procedure has been applied to construct the brown curve in that panel but using the analogous lattices where the small geometrical motifs are randomly placed.
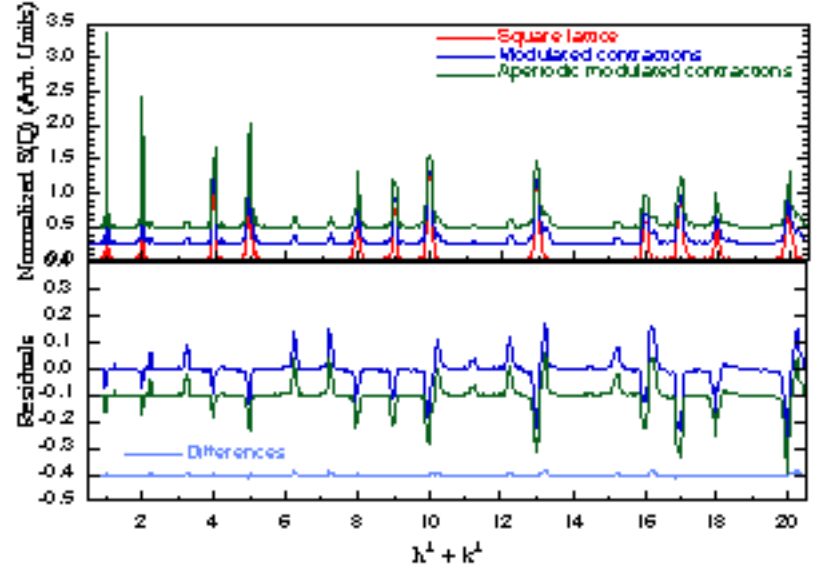

(a) Radial distribution function

(b) Structure factor

Figure 9: RDF and $S(Q)$ for the lattice with a tetragonal domain. See the comments in the caption of figure 7 about how the lower panel has been constructed.
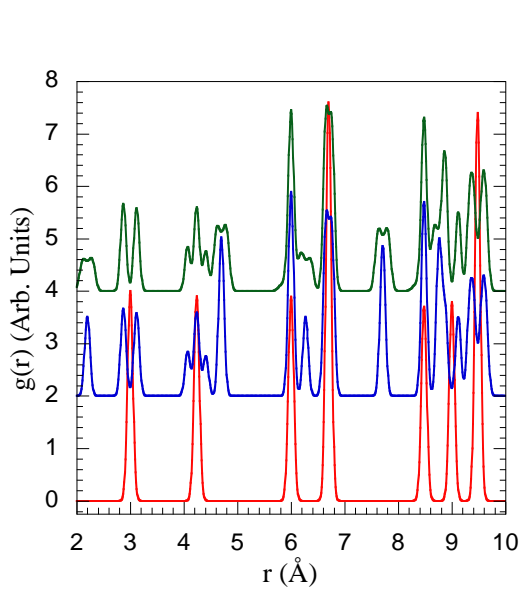
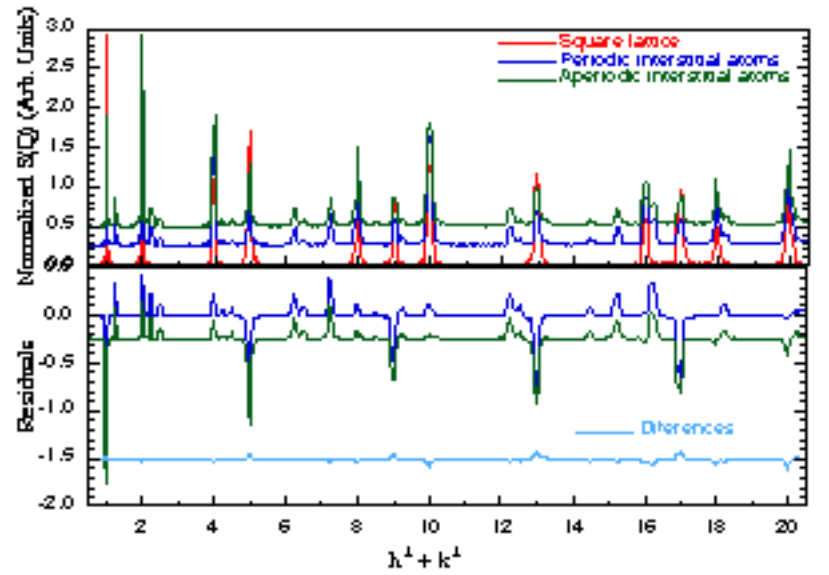(a) Radial distribution function

(b) Structure factor

Figure 10: RDF and $S(Q)$ for the modulated lattices. See the comments in the caption of figure 7 about how the lower panel has been constructed.

(a) Radial distribution function

(b) Structure factor

Figure 11: RDF and $S(Q)$ for the lattices with interstitial atoms. See the comments in the caption of figure 7 about how the lower panel has been constructed.

(a) Radial distribution function
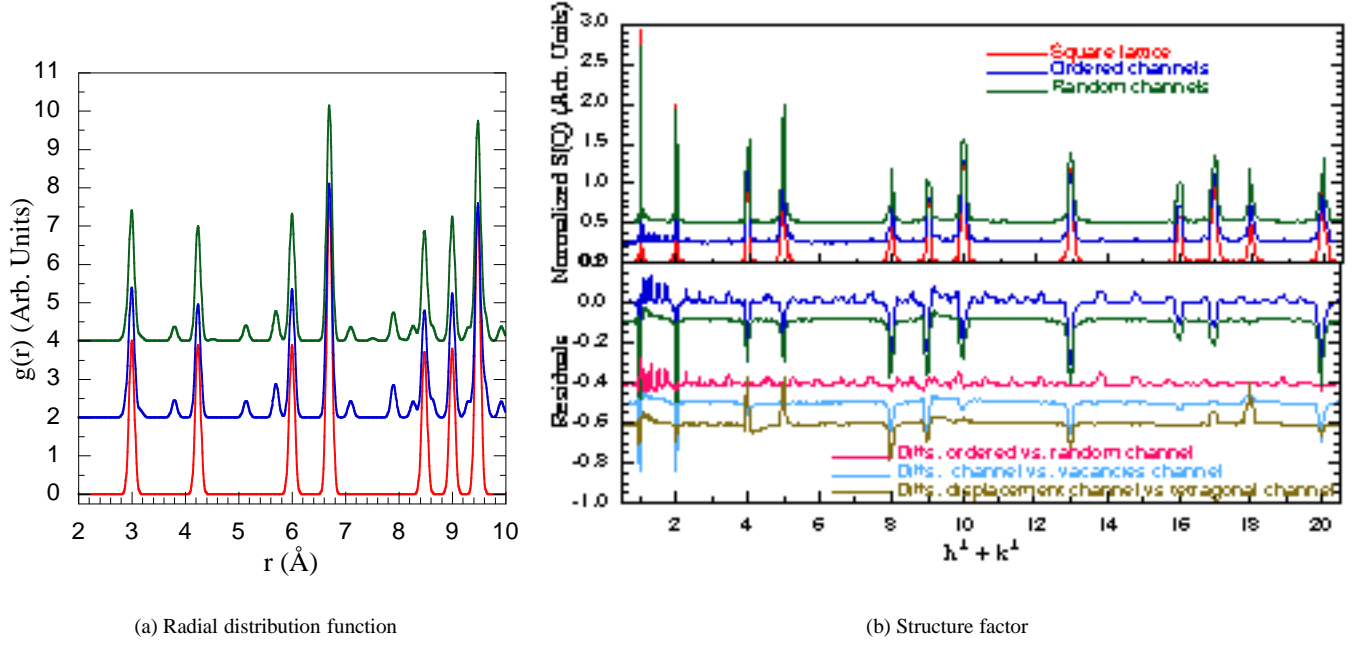
(b) Structure factor

Figure 12: RDF and $S(Q)$ for the lattices with tetragonal distortions forming channels. See the comments in the caption of figure 7 about how the lower panel has been constructed.
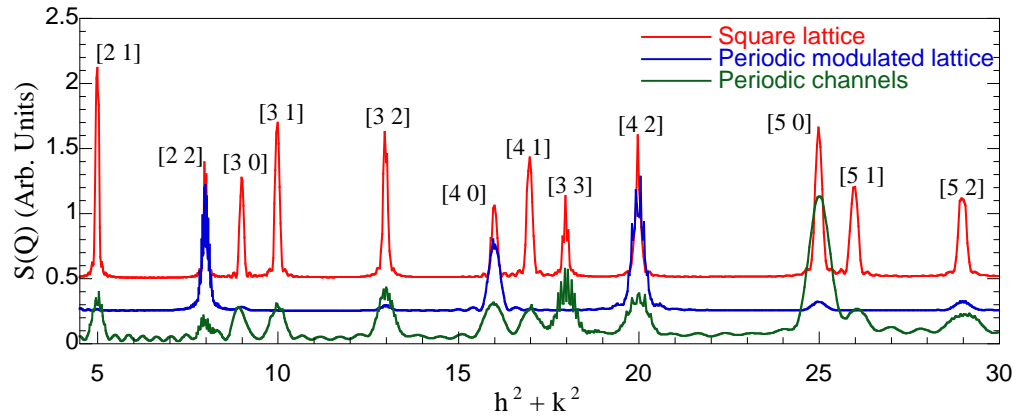

Figure 13: Structure factors for the square lattice, the periodic modulated lattice, and the lattice with periodic tetragonal channels. In this figure the normalization factors for the different lattices are different, as we are only interested in the positions of the peaks of the distorted lattices compared with the positions of the Bragg reflections of the square lattice.